Detecting and Avoiding Unstable Operation of Autothermal Reactors

An on-line procedure is developed that uses estimates of the dominant eigenvalues of a reactor-exchanger system to detect impending unstable operating behavior. In the event reactor stability is threatened, changes are made in the reactor's nominal operating state through a procedure that ensures the attainment of an acceptable degree of relative stability. The reactor stability assessment is made through estimation of closed-loop eigenvalues derived from a physically-based dynamic model. The guiding of the reactor to safe and stable conditions is carried out through a multiloop control system that receives optimal process setpoints found from an interative search. Experiments were made on a laboratory autothermal reactor system to assess the correspondence of the predicted and observed degrees of reactor stability.

Paul H. Gusciora
Alan S. Foss
Department of Chemical Engineering
University of California
Berkeley, CA 94720

Introduction

A fixed-bed autothermal reactor can become less stable over time as it experiences changes in the feed concentration, the catalyst activity, or the feed flowrate. For substantial changes, operating conditions must be adjusted in order to continue operating safely. This work is concerned with maintaining reactor operability in the face of such disturbances. The major concern is smoothly guiding the process to setpoints that provide an acceptable degree of stability and that are optimal at that instant of time.

Maintaining operability and stability in the face of large process disturbances has always been a concern of engineers in process operations, but the development of strategies has received little attention in the literature. van Heerden (1953, 1958) pioneered the steady-state analysis of the autothermal reactor for the purposes of design. Orcutt and Lamb (1960), Baddour et al. (1965), and Luss and Amundson (1967) studied the stability of the autothermal system and gave insight to the operations problems, but did not provide strategies for responding to disturbances. A recent work by Gilles (1986), however, develops a strategy for detecting and curbing runaway conditions, but it relies on a tracking and analysis of a runaway process variable. Several workers have developed means of regulating process outputs for relatively small disturbances. Bonvin et al. (1983), Wong et al. (1983), and McDermott and Mellichamp (1983) developed methods for stabilizing the autothermal system at an unstable steady-state and McDermott et al. (1984) investigated multiloop self-tuning controllers for both stable and unstable steady states.

This work departs from those approaches and extends earlier work by Metchis and Foss (1987) that was directed toward averting extinction of the autothermal condition. This work reports a more general approach than that of Metchis in assessing the stability of an operating reactor. On-line estimates of eigenvalues of a mathematical model of the reactor are the primary indicator of the degree of processes stability and are used in an optimization procedure that guides the reactor to other acceptably safe but still optimal conditions. Similar objectives were pursued by Metchis, but the stability index was couched instead in terms of a *temperature margin,* the difference between the temperature of the reactant feed and a temperature near the *blow-off temperature* of autothermal reactors. Stephens and Richards (1973) used a similar index of reactor stability in an investigation of ammonia synthesis converters. In those investigations as well as this, operation is held close to the *blow-off point* because of the region's importance as the economic optimum in commercial ammonia and methanol synthesis reactors (Baddour et al., 1965). Assessment of reactor stability under operation in this region is necessary because process disturbances and changes in operating conditions (directed, for example, by a process optimizing procedure) can cause the reactor to slide to extinction or to suffer growing oscillations (Metchis, 1982; Gusciora, 1986). Our major objective is to make such an assessment of instability quickly without waiting for the pro-

Correspondence concerning this paper should be addressed to A. S. Foss.
The present address of P. H. Gusciora is: Chevron Corporation, Engineering Technology Department, P.O. Box 1627, Richmond, CA 94804.

cess to exhibit runaway or oscillatory behavior and to conduct the process smoothly to new conditions.

A graphical description of a system to carry out these procedures is shown in Figure 1. The eigenvalue estimates determined in element 3 of the figure are used in stability constraint functions (element 4) of an optimization procedure that finds the best but acceptably stable process setpoints. A multiloop control system in element 1 coordinates the process adjustments.

There were several major efforts needed to develop this system. The reactor model, from which we sought rapid estimates of eigenvalues, had to be a physically-based model because it was necessary to determine also the eigenvalue sensitivity to setpoint changes. Because such models for fixed-bed reactors consist of several partial differential equations, both numerical and physically motivated approximations are needed to render the model tractable and practical for on-line use. These reductions were accomplished through development of a hybrid Taylor dispersion approximation and several numerical approximation techniques. The optimization task is a straight-forward minimization of a nonlinear profit function under nonlinear constraints. Fortunately no new development was needed here; however, implementation was not effortless. The multiloop control system was developed as a part of this project to regulate various process variables and to coordinate the movement of others to new values. It conveniently implements a wide variety of control functions and arithmetic operations. A description of a version of this control program has been given by Foss (1987). Finally, the laboratory reactor system in element 2 of Figure 1 served to test the workability of portions of the full system.

Fixed-Bed Reactor and Reactor Model

The laboratory reactor used in this work and its control system is shown in Figure 2. The exothermic reaction between oxygen and hydrogen occurs on catalyst particles in two reactor beds. The two beds are coupled to an external heat exchanger that preheats the feed to ignition temperature. It is this feedback of heat that can lead to instability of the reactor. The reactor was capable of operating under conditions that exhibited three steady states. The high-conversion (high-temperature) steady state was the one of interest in this work; it was sometimes stable, sometimes unstable. Of the several control system setpoints shown in Figure 2, the two most important are the bed 1 inlet temperature ($T_{1,in}$) and the quench flow rate (Quench); these two are used by the optimization procedure to guide the reactor to stable operating states. A more complete description of the experimental apparatus and operating conditions is given by Metchis and Foss (1987).

A finite-dimensional state-space representation of the current reactor behavior is needed to obtain the eigenvalues. Locally linear models of this type have been used in many investigations of reactor dynamics and control (e.g., Michelsen et al., 1973; Bonvin et al., 1983); they are of the form:

$$\frac{dx}{dt} = \boldsymbol{A}x + \boldsymbol{B}u$$
$$y = \boldsymbol{C}x + \boldsymbol{D}u \tag{1}$$

In our case, the state vector x consists of temperatures at several locations throughout the catalyst beds and heat exchanger. The eigenvalues of the matrix A are computed online because they change with operating conditions as elements of the A matrix change with the nominal reactor steady state.

The derivation of a model of this form from the original mass and energy balances has been fully described in the literature (e.g., Michelsen et al., 1973; Silva et al., 1979; Metchis and Foss, 1987). Central to the development is the use of the orthogonal collocation approximation of the spatial variations of temperatures and concentrations throughout the reactor. The normalized mass and energy balances presented in the references cited are given here to show their form and content:

Fluid material balance

$$v \cdot \frac{\partial Y_f}{\partial z} = -Y_f \cdot R(K, T_p); \quad Y_f(0, t) = Y_{in}(t) \tag{2a}$$

Fluid energy balance

$$v \cdot \frac{\partial T_f}{\partial z} = H_p \cdot [T_p - T_f] + H_w \cdot [T_w - T_f]; \quad T_f(0, t) = T_{in}(t) \tag{2b}$$

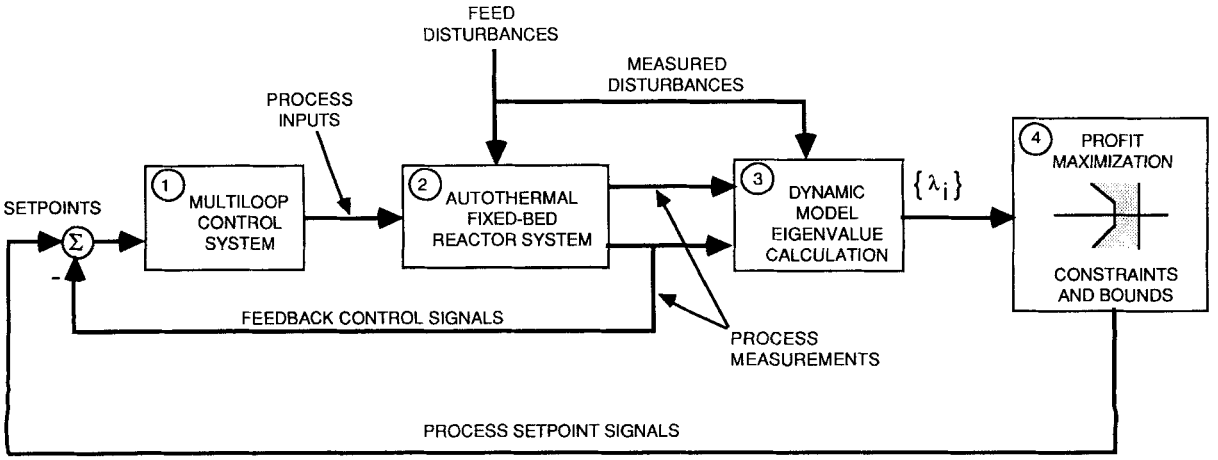

Figure 1. Conceptual diagram of system components used to detect and avoid unstable operating conditions.

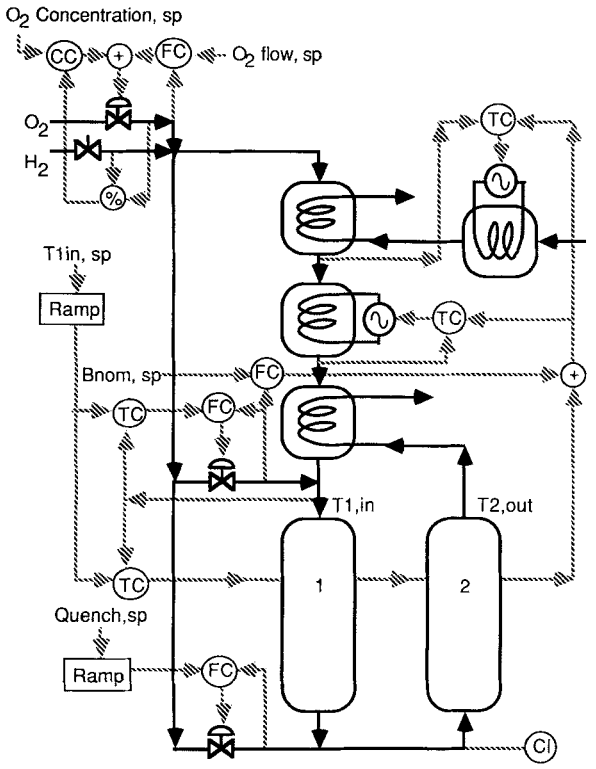

Figure 2. Two-bed autothermal reactor and its regulatory control system.

Particle energy balance

$$\delta \cdot \frac{\partial T_p}{\partial t} = Y_f \cdot R(K, T_p) + H_p \cdot [T_f - T_p]; \quad T_p(z, 0) = T_{p,ss}(z) \quad (2c)$$

Wall energy balance

$$\frac{\delta}{\gamma} \cdot \frac{\partial T_w}{\partial t} = H_w \cdot [T_f - T_w] + H_e \cdot [T_e - T_w]; \quad T_w(z, 0) = T_{w,ss}(z) \quad (2d)$$

Reaction rate temperature dependence

$$R(K, T_p) = K \cdot \exp\left(\frac{E_{\text{ref}} \cdot T_p}{T_p + T_{\text{ref}}}\right) \quad (3)$$

State-space equations of the form of Eq. 1 were derived from these by local linearization about a nominal operating state and application of the orthogonal collocation approximation (Gusciora, 1986). For each bed, six internal collocation points and both end points were needed. After incorporating the boundary conditions associated with the feed stream, there were 14 ordinary differential equations for each bed, containing seven state variables for the catalyst temperatures and seven state variables for the reactor wall temperatures throughout the bed. The double-tube heat exchanger was modeled in a similar way using four internal collocation points, resulting in seven state variables for exchanger wall temperatures when all boundary conditions were applied and a noninfluential state removed. The junctions between the beds and between the exchanger and reactor beds were modeled simply as constant gain elements.

The full reactor-exchanger state-space model consists of 35 state variables. It was determined early that an A matrix of order 35 was far too large to treat online for calculation of eigenvalues. The excessive size of the state vector arises from the appearance of temperature elements for both the catalyst and reactor wall in each bed. These temperature state variables appear because the model accounts for finite rates of heat exchange between the fluid and these stationary thermal masses. Those heat interchanges, however, can be modeled in an approximate way with a single mean temperature through use of the Taylor dispersion approximation (Rosenbrock and Storey, 1966; Gould, 1969). A hybrid of the classical Taylor dispersion model was made (Gusciora, 1986; Gusciora and Foss, 1988) that transforms the system of first-order partial differential equations (Eqs. 2) to a second-order partial differential equation of the convected diffusion type in a single mean temperature. The number of state variables for each reactor bed is thus cut in half. Hybridization involves a direct incorporation of the rate of heat loss and heat generation in the Taylor dispersion model of a nonreactive bed and the coordinated use of the reactant balance (Eq. 2a) in evaluating the heat generation rate. Part of the approximation procedure involves matching of three moments of the impulse response to determine values of three empirical coefficients of the hybrid model, a very rapid calculation as described by Gusciora and Foss (1988). In addition, all of the state variables for the heat exchanger were discarded because frequency response analyses showed it to behave very much like a pure gain relative to the reactor beds.

Upon application of the collocation approximation to the hybrid model, one is led to a total reactor-exchanger system model of the form of Eq. 1 having eight to 12 state variables (corresponding to one's choice of four to six state variables for each bed). The dominant eigenvalues of an eight-state model showed a good match with those of the full 35th-order model. For convenience in implementing calculations online, the same number of collocation points were used in spatially discretizing both beds, even though some cases permitted as few as three states in the reduced-order model of the first bed.

The hybrid-TDM developed here achieves the same order of reduction as the modal reduction techniques described by Bonvin and Mellichamp (1982) and Litz (1981). However, those reduction techniques require calculating eigenvalues and eigenvectors or singular values and principal vectors of the original model. As described by Gusciora and Foss (1988), the hybrid-TDM requires only the moments of the original model, which can be calculated much more rapidly. The overall computation time for the eigenvalues of the two-bed reactor-exchanger system is reduced by a factor of 20–40 for the hybrid-TDM scheme, compared to an overall reduction of at most 2–3 for modal reduction schemes applied to the individual reactor beds.

Systems for Optimization and Control

Optimization functions

An optimization procedure was used to drive the process towards desirable steady states. The objective function of this procedure attempts to account for production revenue, energy costs, and catalyst deactivation. In terms of dimensionless vari-

ables the objective is:

$$\text{Minimize } [\text{Cost}P \cdot v_{\text{feed}} \cdot (Y_{\text{feed}} - Y_{2,\text{out}}) + \text{Cost}E \cdot v_{xs} \cdot (T_{xs,in} - T_e) + \text{Cost}D1 \cdot T_{1,\text{out}} + \text{Cost}D2 \cdot T_{2,\text{out}}] \quad (4)$$

where

$\text{Cost}P$ = cost of production < 0

$\text{Cost}E$ = cost of energy > 0

$\text{Cost}D$ = cost of catalyst deactivation > 0

The first term, the production revenue, accounts for possible variation of the total feed flow and conversion. The second term accounts for the energy cost, which is proportional to the amount that the feed has to be heated above ambient temperature by the auxiliary heaters. The third term accounts for catalyst deactivation and reverse reaction. The deactivation term is included to simulate the deactivation that occurs in industrially important systems, even though the decline of catalyst activity was slow here. The assumption is that high bed temperatures cause deactivation, and the highest bed temperature occurs at or near the bed outlet, thus motivating the use of that temperature in the objective function. To simulate the effect of a reversible reaction on the production rate, we add more weight to the high temperatures in the beds by increasing $\text{Cost}D$, thus keeping the objective simple.

This cost function is simplistic, but a more complicated expression would obscure the main thrust of this work. The main effect is to drive the process towards the lowest possible bed-1 inlet temperature, near the blowoff point, which is believed by some authors to correspond to the economically optimum operating point. The objective function is dimensionless, but the solution depends on the ratio and not the absolute value of the cost coefficients.

The minimum of this function is found by varying $T_{1,in}$ and Quench subject to process constraints and stability constraints. The first set of process constraints are simply upper and lower bounds for each setpoint or optimization decision variable:

$$T_{1,in} - T_{1,in,LO} \geq 0 \quad (5a)$$

$$-T_{1,in} + T_{1,in,HI} \geq 0 \quad (5b)$$

$$\text{Quench} - \text{Quench}_{LO} \geq 0 \quad (6a)$$

$$-\text{Quench} + \text{Quench}_{HI} \geq 0 \quad (6b)$$

Two constraints limit the maximum allowable temperature in the beds:

$$-T_{1,\text{out}} + T_{1,\text{out},HI} \geq 0 \quad (7a)$$

$$-T_{2,\text{out}} + T_{2,\text{out},HI} \geq 0 \quad (7b)$$

One further process constraint limits the maximum amount of unconverted reactant:

$$-Y_{2,\text{out}} + Y_{2,\text{out},HI} \geq 0 \quad (8)$$

This effectively forces the system to the upper, high-conversion steady state.

To these process constraints are added the stability constraints, which, in our approach, constrain the closed-loop system eigenvalues to the left of an arbitrary contour in the complex plane. We use a piece-wise linear contour like that of Figure 3. This contour can be constructed from the intersection of the two simpler allowable regions shown in Figure 4. The simple regions are parameterized by two constants q_r and ζ. The damping factor ζ is defined by analogy with second-order systems. Figure 4 shows that the complex plane is divided by lines of constant damping factor ζ which intersect at q_r on the real axis. For complete analogy with second-order systems q_r would be identically zero, but in this work setting q_r nonzero allows the flexibility to compensate for a certain amount of plant-model mismatch. For additional flexibility to accommodate modeling error, two constraints, parameterized by two (q_r, ζ) pairs, are applied to each closed-loop and, if desired, each open-loop eigenvalue. Thus the allowable region is the intersection of two simpler regions. Alternatively, the forbidden region is the union of two simpler forbidden regions. Inclusion of constraints on the open-loop eigenvalues in addition to the closed-loop eigenvalues would be recommended if one is concerned about reactor system stability upon failure of the control system.

Algebraically, the allowable region is bounded by the point-normal equation of the lines with damping factor ζ passing through the point $\boldsymbol{q}$:

$$\boldsymbol{p}^T \cdot [z - \boldsymbol{q}] \geq 0 \quad (9a)$$

$$\boldsymbol{p}(\zeta, z)^T = [-(1 - \zeta^2)^{0.5}, -\zeta \cdot sgn(z_i)] \quad (9b)$$

$$\boldsymbol{q} = (q_r, 0)^T \quad (9c)$$

Here the complex plane is a Euclidean two-space: $z = (z_r, z_i)^T$. Figure 4 shows the geometric interpretation of these equations. The left side of relation 9a is positive for points z on the acceptable side of the constraint. The normal $\boldsymbol{p}$ of the constraint boundary is a function of both the damping factor ζ, and the position of the point z above or below the real axis.

The allowable regions and the eigenvalues of the model are symmetric with respect to the real axis. Because of symmetry, the constraints corresponding to eigenvalues with negative imaginary parts are redundant. If they are eliminated in order to reduce the total number of constraints, problems can occur as

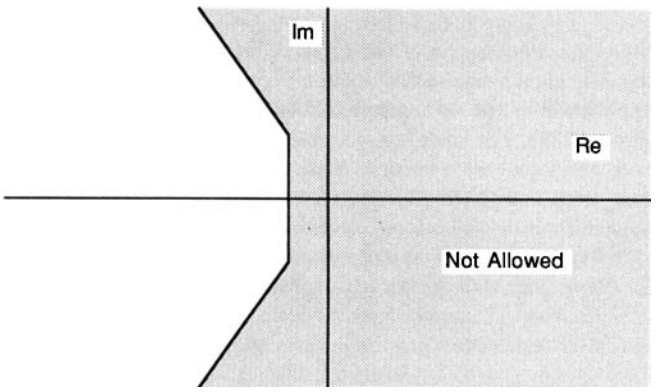

Figure 3. Typical eigenvalue constraints.

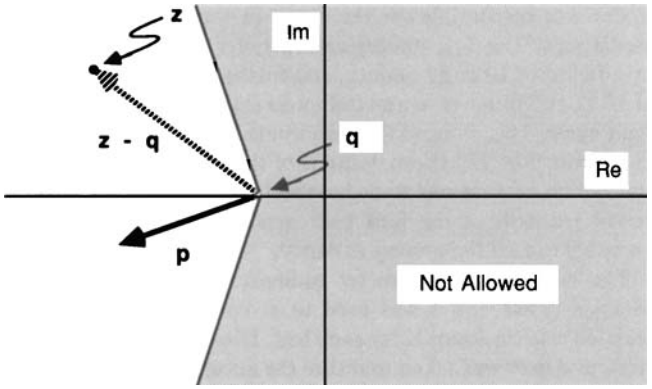

Figure 4. Geometric interpretation of eigenvalue constraint relation: $p^T \cdot [z - q] \geq 0$.

the numerical optimization proceeds. If two real eigenvalues should collide and split off to form two complex-conjugate eigenvalues, the number of constraints would be reduced by one. Conversely, if two complex-conjugate eigenvalues should coalesce on the real axis and split off into two real eigenvalues, the number of constraints would be increased by one. Currently available optimization software cannot handle changing numbers of constraints but can handle redundant constraints fairly well.

Another possibility for reducing the number of optimization equations is to constrain only the dominant eigenvalue, say the rightmost one having the most positive real part. Unfortunately, the selection of an eigenvalue from the set results in a constraint that does not have a continuous first derivative. Currently available optimization packages have difficulty with functions that do not have continuous first derivatives. For these reasons, all of the eigenvalue constraints are presented to the optimization routine. Thus, when the constraints for the 13 closed-loop eigenvalues are appended to the process bounds, there are $7 + 2(13) = 33$ total constraints, since there are two linear segments defining the stability boundary. If the constraints for the 12 open-loop eigenvalues are included also, the total number of constraints would increase by 2(12) to 57.

Derivatives of optimization functions

Most efficient numerical optimization techniques require derivatives of the objective function and constraint functions. Because Eqs. 4–9 depend on the calculated output of the model and cannot be differentiated analytically, the derivatives were computed by finite difference. The constraint and objective functions are evaluated at the current values of $T_{1,in}$ and Quench and then at conditions where $T_{1,in}$ and Quench are perturbed slightly. Although Eqs. 5–6 can be differentiated analytically, it was simpler to include them in the general case.

The computation of the derivatives of the eigenvalues appearing in equation 9a is not so straightforward. The eigenvalue subroutines return a vector containing the set of eigenvalues $\{\lambda\}$ of the matrix A, with no guaranteed order in the set. Small changes in the elements of the A matrix can produce large changes in the ordering of the eigenvalues, even though they produce small changes in the eigenvalues themselves. This difficulty was overcome by pairing the closest eigenvalues in each set. The L_1 (Frobenius or sum of absolute values) norm was used to compute distance as it is more rapidly computed than the L_2 (Euclidian or square root of sum of squares) norm and avoids problems with floating-point underflow. The computation of the paired finite-difference takes much less time than the computation of the base-case and perturbed eigenvalues. An alternative procedure for computing derivatives of eigenvalues based on an analytical expression was found to require greater precision in the eigenvectors, eigenrows, and the finite-difference approximation to the derivative of the A matrix than was available from single-precision arithmetic.

Optimization algorithm

Powell's (1978a,b) augmented Lagrangian method, also known as SQP (sequential quadratic programming) (Luenberger, 1983), was chosen as the nonlinear optimization method to solve Eqs. 4–9 for the two optimum setpoints $T_{1,in}$ and Quench. This method was chosen because it has strong global convergence properties and retains some information about the local nonlinear behavior of the functions so as to minimize the number of function evaluations. Most importantly, the method is included in several program libraries. The greatest problems in converting the code to single precision on our process minicomputer lay with the underlying QP (quadratic programming) and phase-1 LP (Linear Programming) code, which did not seem to be structured to handle redundant constraints generated by the eigenvalue constraints.

The optimization is carried out by a program that computes in turn: the steady-state profiles, reduced-order linear model, eigenvalues, perturbed steady-state profiles, perturbed eigenvalues, constraints, and derivatives. It is iterated until the optimization subroutine returns new $T_{1,in}$ and Quench setpoints for the regulatory control system.

Regulatory control system

The multiloop regulatory control system shown in Figure 2 consists of a structure of cascaded PI (proportional-integral) loops and is similar to that used by Metchis and Foss (1987). Controlling the inlet temperature is divided among two sections: short-term and long-term. A short-term $T_{1,in}$ control is accomplished by manipulating the setpoint to a rapid bypass-flow control loop. The cascade isolates the temperature control loop from pressure disturbances and valve nonlinearity. Long-term $T_{1,in}$ control is provided by a slow temperature controller cascaded onto either the startup-heater temperature controller or the auxiliary-heater temperature controller.

The bypass flow rate is driven to its nominal value by a very slow controller which sums onto the setpoint of the startup-heater or auxiliary-heater controller. This configuration is substantially different from Metchis' "parasitic" nominal-bypass controller and was considerably easier to tune. The inlet-temperature setpoint passes through a ramp (or velocity) filter which limits the rate of change of $T_{1,in}$. The quench-flow-rate setpoint also passes through a ramp filter before introduction into a rapid regulatory loop. The ramp (or velocity) filters were easier to tune than Metchis' first-order setpoint filters. The feed concentration is regulated by manipulating oxygen flow rate. This control loop is required by the construction of the laboratory process and has no industrial analogue. The feed-flow control loop was used during calibration.

All of the control loops use digital single-variable PI control algorithms. A table-driven on-line control program was used in

controlling the process and greatly aided the testing and operation of the process and the regulatory control structure. The control loops were tuned using a combination of theoretical analysis, step testing, and heuristic adjustment, starting from settings inherited from Metchis (1982, 1987) and Lappinga (1984a, b).

Experimental Tests

Test of model fidelity

Instability of the process was difficult to demonstrate with our experimental apparatus. Further, the laboratory process proved to be more stable than the approximate model. Metchis (1982, 1987) noted this fact in his work with the same process. Stephens and Richards (1973) also noted that the ammonia synthesis converter they studied was more stable than their model predicted.

Nevertheless, oscillations with very small damping were observed in the controlled process. Figure 5 shows oscillations in the temperatures that were induced by a feed concentration pulse. The operating conditions were similar to those reported by Metchis and Foss (1987); differences may be found in Gusciora (1986). It is observed that the mean of the oscillations of bed 2 outlet temperature falls below the initial steady-state value, and the amount of heat available to sustain the process falls as well. The $T_{1,in}$ controller responds by reducing the bypass flow rate to keep $T_{1,in}$ at its setpoint. It was thought that the $T_{1,in}$ controller was responsible for the decay in the magnitude of the oscillations. The $T_{1,in}$ stabilizing controller gains were reduced by a factor of 10 at 89 minutes and further reduced by a factor of 10 at 106 minutes in an attempt to stabilize the process at a limit cycle. This reduced the magnitude of the control effort on the bypass flow, but the magnitude of the oscillations decreased and the process seemed to be headed toward extinction. A slow downward drift of the feed hydrogen flow rate by about 9% probably caused the process to decay.

The steady-state parameter estimation procedure used by Metchis (1982, 1987) was used to arrive at estimates of the reaction rate constants K for each bed. These are critical parameters, and care was taken to insure the accuracy of steady-state temperature-profile predictions when these parameters were used in the model. The calculated eigenvalues were sensitive to the parameters and the measurement accuracy, but no more so than the steady-state model predictions.

Figure 6 shows the eigenvalues of the linearized process model for these conditions. This figure takes advantage of the symmetry of the eigenvalues with respect to the real axis by presenting only the top half plane. Note that three calculated open-loop eigenvalues, labeled $O1$ and $O2$, are in the right-half plane, indicating an unstable process. It seems that the $T_{1,in}$ controller stabilizes the system somewhat by moving the eigenvalues toward the left. The two complex closed-loop eigenvalues, labeled $C1$, are closer to the real axis, but still in the right-half plane. The process real eigenvalue ($O2$) has split with the con-

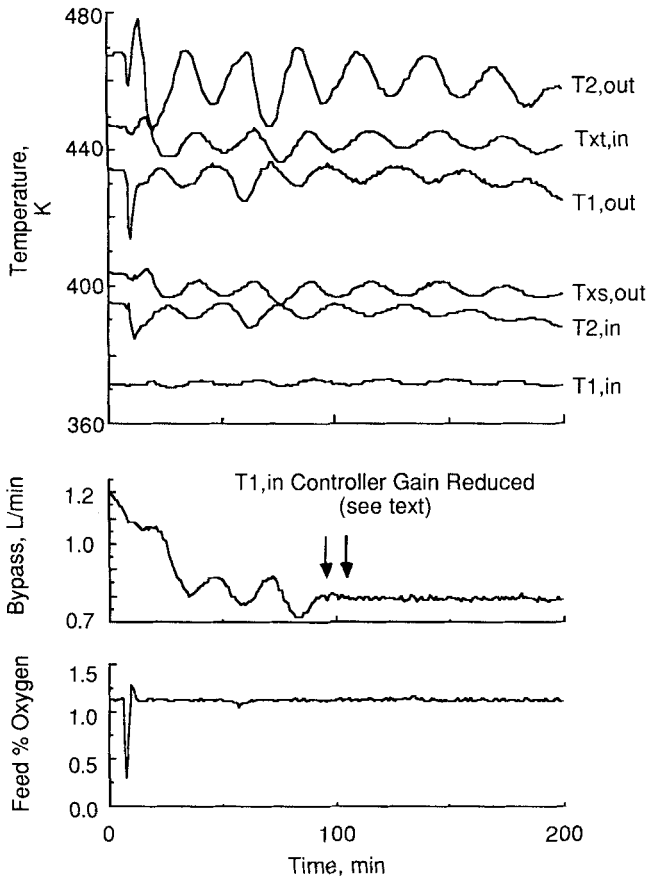

Figure 5. Experimentally observed damped oscillations in the controlled reactor induced by a negative pulse in feed concentration.

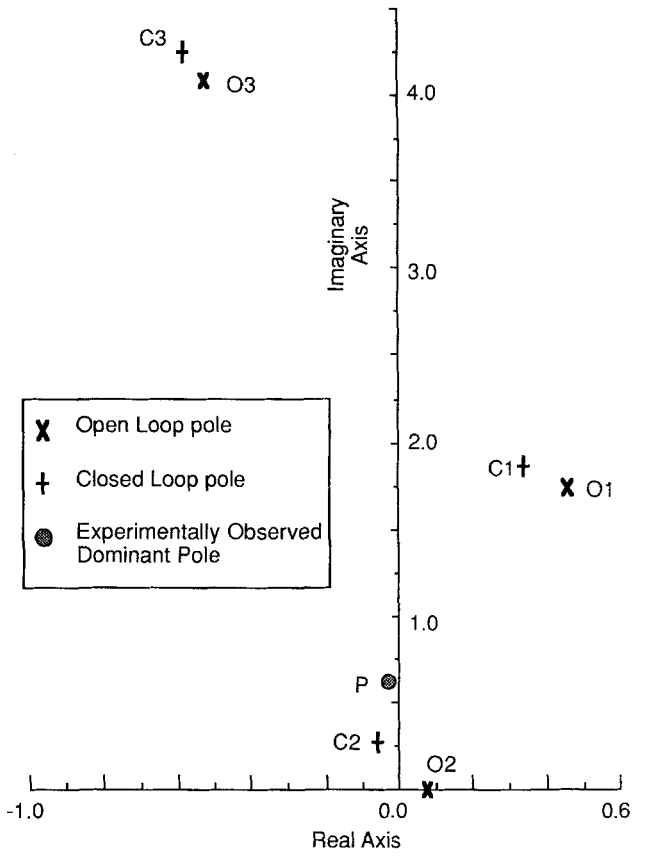

Figure 6. Locations of dominant model eigenvalues and experimentally observed system pole under conditions of Figure 5.

troller integrator pole to form two complex closed-loop eigenvalues, labeled $C2$, that are just to the left of the imaginary axis.

Figure 6 also shows a complex pole P corresponding to the experimentally observed oscillations in Figure 5. The oscillation has a 30-minute period and a 0.8 damping ratio. Using the reference time $t_{ref} = 170$ s, this translates to the pole labeled P at $(-0.02 \pm 0.62i)$ with a damping factor $\zeta = 0.035$. This pole is closest to the left-half-plane eigenvalue $C2$ at $(-0.045 \pm 0.30i)$, and suggests that the right-half-plane eigenvalue $C1$ at $(0.24 \pm 2.0i)$ is the result of modeling error.

Neglected thermal dynamics at the interbed joints is the most likely source of modeling error. An expanded view of the oscillations shows that there is eleven minutes of lag between the bed 2 outlet temperature and the bed 1 inlet temperature but less than one minute of lag between the inlet of the heat exchanger and the outlet of the heat exchanger (Gusciora, 1986). This confirms the validity of treating the heat exchanger as a pure gain but reveals the error in modeling the junctions similarly. Although larger systems should have proportionally smaller interunit capacitances, neglecting dynamics of pipes connecting process units has caused significant error in physically-based models of industrial pilot plants (Leonard, 1986). Since the variation of the joint dynamics with respect to inlet temperature or quench flow rate is much smaller than the variation of the reactor bed dynamics, the derivatives of the eigenvalues with respect to the process setpoints should not be greatly affected by this modeling oversight.

We argue here that eigenvalue $C2$ of Figure 5 is the authentic dominant eigenvalue that demands constraint during operations and that eigenvalue $C1$ is merely an artifact of modeling error. The right-half-plane closed-loop eigenvalue $C1$ results from positive feedback around the reactor beds by the heat exchanger. If the pure gains of the heat exchanger and the joints are replaced by first-order lags, the feedback around the reactor beds at high frequencies will be attenuated, and the eigenvalue will move toward the left (more stable) and to smaller imaginary parts (longer period). The left-half-plane closed-loop eigenvalue $C2$ results from both positive feedback around the beds by the heat exchanger and negative feedback around the heat exchanger by the PI controller. If the pure gains are replaced by first-order lags, the feed-back at high frequencies will be attenuated, and the predicted controller performance will deteriorate. The net result is that the open-loop eigenvalue $O1$ at $(0.8 \pm 0.0i)$ will move to the left, and the closed-loop eigenvalue $C2$ will move toward the imaginary axis. If this is the case, the closed-loop eigenvalue at $C1$ is an artifact of approximating the joint dynamics by pure gains in the model. We conclude from this that the model eigenvalue $C2$ is the important eigenvalue for closed-loop stability.

Optimization tests

Several tests of the optimization procedure were made to determine its computational workability, its response to changing feed concentration, and its sensitivity to some of the cost coefficients and constraint parameters. The optimization problem consists of finding values of $T_{1,in}$ and Quench flow rate (i.e., the two control system setpoints) that minimize the objective function (Eq. 4) subject to the 33 constraints previously described. Since the minimization algorithm is iterative, a sequence of the ($T_{1,in}$, Quench) coordinates are produced, and the particular trajectory traversed in any one case will depend on the parameters used in the objective and constraint functions.

The cost weighting factors in the objective function (Eq. 4) were set to reflect the usual competition between production rate and the deleterious effects of high bed temperatures. Energy costs were not considered significant. Because temperatures are higher in bed 2, the weights there were set equal to or larger than those of bed 1. Values of the catalyst deactivation cost Cost$D2$ were set to 1 and 2 in the two cases discussed here. The value of Cost$D1$ was set at 1. These compare with the production rate cost Cost$P = -1$.

Parameters for the stability contour were chosen so that the important eigenvalue near $C2$ of Figure 6 would be constrained, but the eigenvalue near $C1$ (the artifact resulting from modeling error) would not be constrained. Figure 7 shows a typical contour. The need to fashion a contour of such shape illustrates the value of designing a stability criterion incorporating multiple segments.

Bounds on the setpoint variables $T_{1,in}$ and Quench were set to reflect the maximum and minimum values achievable by allowable variations in both bypass and quench flow rates. The high and low $T_{1,in}$ values were selected wide enough (400 K and 350 K) such that they were not expected to become active. The high and low bounds on Quench were set at 3 L/min and 1 L/min and were expected to become active. The upper bounds on bed outlet temperatures were set high to preclude those constraints becoming active because of our interest in observing the effect of

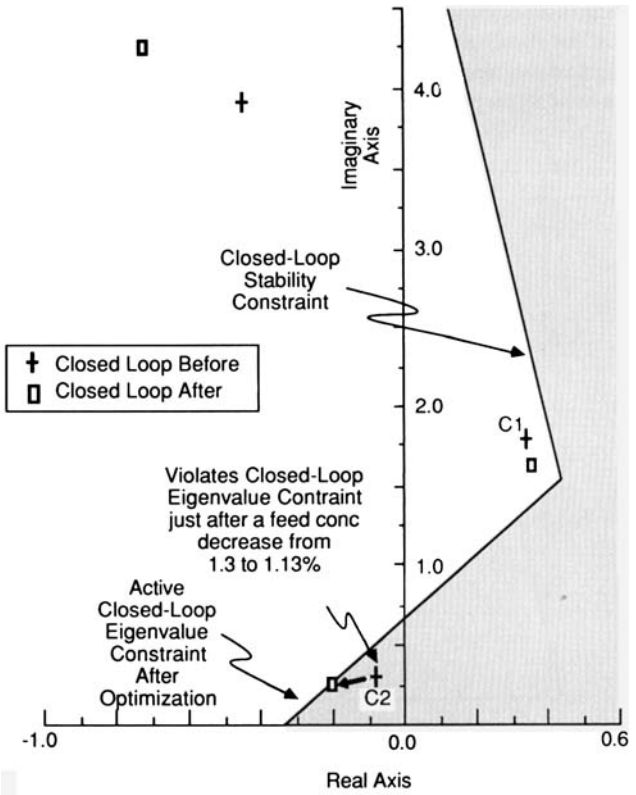

Figure 7. Orientation of the stability constraint relative to the estimated closed-loop eigenvalue locations before and after a reduction in feed concentration from 1.3% to 1.13%. Cost$D2$ = 2.

those temperatures on the optimizing trajectory through their influence in the objective function. Finally, the upper bound on the effluent reactant concentration was set at 0.03 (dimensionless) to insure that the minimization procedure kept reactor conditions in the region of the high-conversion steady state.

With these parameters, we can observe how the system guides the reactor from an unstable state to a new state that is stable and optimum. The unstable condition in this example is brought on by a decrease in feed concentration from 1.3% to 1.13%. The situation regarding the two optimization variables and the reactor stability just before and immediately after the concentration decrease is shown in Figures 7 and 8. The starting state is a constrained optimum state (determined by application of the algorithm) at which the Quench rate and dominant closed-loop eigenvalue reside at constraints. Just after the feed concentration decrease, the dominant eigenvalue $C2$ finds itself in the forbidden region, as indicated in Figure 7. The optimization procedure proceeds to direct the reactor's two setpoints to the new optimum state A of Figure 8 by moving along the upper bound of Quench flow and forcing the dominant closed-loop eigenvalue to the stability boundary. The bold line in Figure 7 shows the movement of the eigenvalue, and the sequence of iterations to the optimum is shown by the arrows in Figure 8. The move to the new constrained optimum required only three evaluations of the objective and constraint functions. Only the final setpoint values are sent to the regulatory controllers.

In the case just described, a large weight (Cost$D2$ = 2) was placed on bed 2 temperature. If that weight is reduced to that of the bed 1 temperature (i.e., Cost$D2$ = Cost$D1$ = 1), we find that another optimum state (B of Figure 8) is attained at which the dominant closed-loop eigenvalue is just on the stability contour but the Quench flow rate now resides at its lower bound. The uniform weighting of bed 2 and bed 1 temperatures may be the most appropriate when temperatures in the beds are nearly the same, as they are at the lower feed concentration. Four function evaluations were needed to arrive at this state. The large excursion of Quench flow between high and low limits results from the linear weighting of bed temperatures used to reflect the cost of catalyst deactivation. If nonlinear weighting were added corresponding, for example, to an exponential dependence of deactivation on temperature, the optimization could terminate at an intermediate value of the Quench rate.

There is some insight to be gained about the optimal solutions by examination of the gradients of the objective and constraint functions at the optimum. For optimum state A, these are shown in Figure 9. The gradients of the two active constraints straddle the gradient of the objective, as they must when two constraints are active at a two-dimensional minimum. If only one constraint is active, the objective and constraint gradients would be parallel. If no constraints are active in an engineering problem of this type, one should be suspicious of the outcome. For the case at hand (i.e., Cost$D2$ = 2), the reduction in concentration results in no substantial shift in the relative orientation of these gradient vectors. There is thus no change in the identity of the constraints active before and after the optimization. A change of the deactivation factor Cost$D2$ from 2 to 1, however, results in an interchange in the orientation of the objective and eigenvalue gradient vectors, which leads to the large excursion in Quench rate to its low bound as shown in Figure 8.

Further investigation of the gradients (Gusciora, 1986) found the first and second dominant eigenvalues to have nearly parallel gradients; it was thus not appropriate to force two eigenvalue constraints to be active at the optimum. Near parallelism was sometimes found between the gradients of the dominant eigenvalue and the outlet concentration constraint. This suggests that

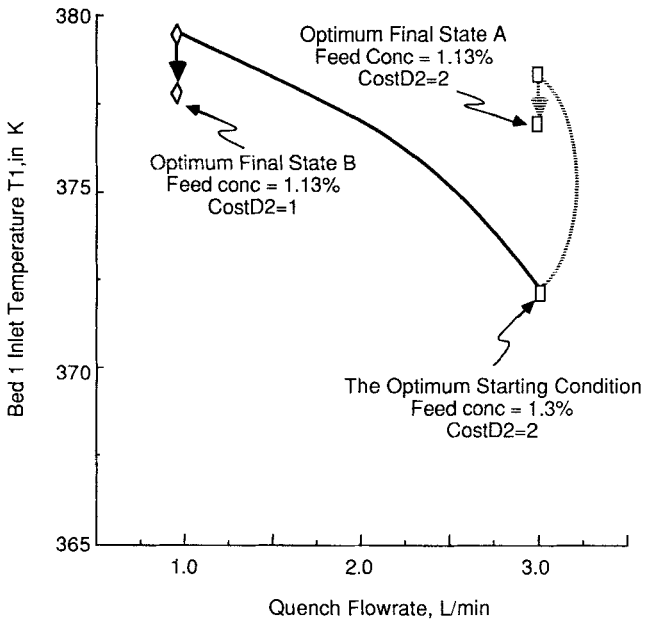

Figure 8. Optimization paths in the $T_{1,in}$-Quench plane upon decreases in feed concentrations from 1.3% to 1.13%.

The square and diamond symbols represent iterations and the arrows show the transitions between them.

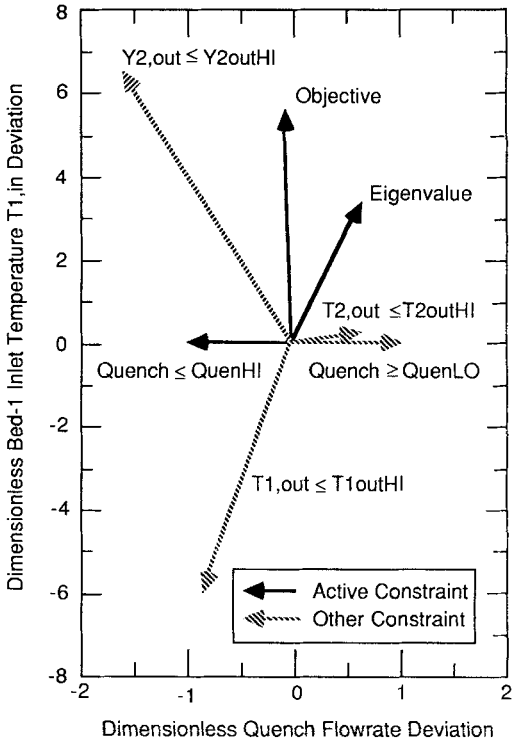

Figure 9. Gradients of objective and important constraint functions at the optimum for 1.13% feed concentration. Cost$D2$ = 2.

if these two are always nearly parallel, online eigenvalue calculation might be replaced by a carefully placed outlet concentration constraint. A further important observation found that the eigenvalue gradient vectors were substantially the same whether or not the $T_{1,in}$ controller was in or out of operation. This suggests that for autothermal processes, the most important feedback loop is established by the process design decision to incorporate a feed-product heat exchanger.

Computational details

The first step of the optimization calculation typically took about 200 seconds, starting from poor guesses of bed profiles and moment matching factors in the hybrid-TDM. Subsequent iterations typically took less time because the profiles from the previous iterations were used as a first guess. In all cases, the optimization subroutine consumed less than 10% of the total time per iteration. Included in the total is the 90 seconds required to calculate six sets of eigenvalues of the reduced-order model, a substantial reduction from the 1,320 seconds required to calculate six sets of eigenvalues of the full 35th-order model. Some cases where only four collocation points were used in the reduced-order reactor model required only 36 seconds for eigenvalue calculation. These results were obtained with a 1975-vintage process computer that is ten times slower than an IBM-XT with a floating-point coprocessor. The optimization program consisted of 10,000 lines of FORTRAN code, used single-precision arithmetic, and required overlays to fit into the available 64 K words of memory.

Usually the optimization converged in three to four function evaluations (steady states, eigenvalues, constraints, derivatives) but sometimes did not converge from all starting points. It tended to make larger moves than necessary and sometimes terminated in a line-search step, especially on the first iteration. This might be corrected by presetting the second derivative of the Lagrangian, but an expedient used here was to restart the optimization from the first step of the line-search algorithm.

Concluding Remarks

The need to protect autothermal reactors from being thrust into an unstable state under abnormal operating conditions has been a major focus of this work. Our approach has been to use a dynamic model of the reactor-exchanger system to obtain a rapid real-time assessment of process stability. It is the dominant eigenvalue of the reactor-exchanger system model that was used for this purpose. Such an approach has the potential of uncovering and correcting an untenable operating state before it becomes apparent in observable variables. In contrast, other methods (e.g., Gilles, 1986) rely on tracking and analysis of the temporal behavior of reactor variables before an assessment of instability can be made.

It is essential that one incorporate flexible and adjustable criteria for stability assessment in any procedure that incorporates a process model. Modeling inaccuracies, both intended and unintended, can result in virtually unanalyzable effects on stability measures such as eigenvalues. Such effects were anticipated here through our use of a translatable and segmental contour to define acceptable regions for the process eigenvalues. The translation and "kinking" of the contour was guided in this work by experimental observation of process response relative to the predictions of the model.

Even with such flexibility incorporated, one is still challenged to develop a reactor model of reasonable fidelity, yet simple enough to be incorporated efficiently in on-line calculations. That challenge is considerable in this application because of the need to represent the dynamic characteristics of a distributed nonlinear process over a range of operating conditions, that is, over a range of setpoints. The modeling technique used here was physically based, and through use of the Taylor dispersion approximation (also physically based) an acceptable model was developed. The time required to accomplish this, however, was much too long. More efficient methods of modeling for these types of applications still need to be developed.

The method employed here to guide the reactor out of an unstable condition to one of stability has been embedded in an optimization procedure. Indeed, the adjustments made in the process setpoints derive from an iterative constrained minimization of an objective function reflecting a process profitability. Among the numerous constraints imposed are the conditions that each of the system eigenvalues lie to the left of the segmented contour in the complex plane, the stability constraints. These and several constraints on process variables were readily incorporated in a standard optimization module.

The use of a modular approach in this and earlier work (Metchis and Foss, 1987) on problems of this complexity is seen to be practicable in both system development and operations. The need to fully confirm the functioning of the several components of such systems indeed makes modularity a practical necessity. Further, the use of modules, such as the dynamic reactor model, its Taylor dispersion approximation, the multiloop control system, and the optimization procedure of this work, makes the entire project accessible to a team of experts. In view of the growing sophistication of the methods now being used in such systems, team work is essential.

Notation

A, B, C, D = matrices of a linear state-space model
Cost(i) = weighing coefficients in objective function, Eq. 4
E_{ref} = activation energy parameter normalized by the reference temperature
H_e, H_p, H_w = heat exchange parameters: reactor wall vs. environment, reactant vs. catalyst particles, and reactant vs. reactor wall
K = normalized reaction rate constant
$\boldsymbol{p}$ = normal vector of eigenvalue constraint
$\boldsymbol{q}$ = vector defining real intercept of constraint contour
Quench = quench flow rate
t = time normalized by nominal thermal transit time
T_f, T_p, R_w, T_e = normalized temperatures of fluid, catalyst particles, reactor wall, and environment
T_{ref} = reference temperature normalized by nominal adiabatic temperature rise
$\boldsymbol{u}$ = input vector in state-space model
v = normalized volumetric reactant flow rate
$\boldsymbol{x}$ = state vector in linear state-space model
$\boldsymbol{y}$ = output vector in state-space model
Y_f = reactant concentration normalized by nominal feed concentration
z = reactor axial coordinate normalized by bed length
$\boldsymbol{z}$ = vector in the complex plane

Greek letters

δ = normalized thermal-wave transit time
γ = particle/wall heat-capacity ratio
λ = eigenvalue of matrix A

Subscripts

e = environment
f = fluid
HI, LO = upper and lower bounds
i = imaginary part of a complex number
in, out = flows entering or leaving
p = catalyst particle
r = real part of a complex number
ss = steady state
w = wall
xs = exchanger shell-side stream
1, 2 = bed 1 or 2

Literature Cited

Baddour, R. F., P. L. T. Brian, B. A. Logeais, and J. P. Eymery, "Steady-State Simulation of an Ammonia Synthesis Converter," *Chem. Eng. Sci.*, **20,** 281 (1965).

Bonvin, D., and D. A. Mellichamp, "A Unified Derivation and Critical Review of Modal Approaches to Model Reduction," *Int. J. of Contr.*, **35**(5), 829 (1982).

Bonvin, D., R. G. Rinker, and D. A. Mellichamp, "On Controlling an Autothermal Fixed-Bed Reactor at an Unstable Steady State: I, II, III," *Chem. Eng. Sci.*, **38**(2), 233, 245, 607 (1983).

Douglas, J. M., J. C. Orcutt, and P. W. Berthiaume, "Design and Control of Feed-Effluent Exchanger-Reactor Systems," *Industrial and Engineering Chemistry Fundamentals,* **1,** 253 (1962).

Foss, A. S., "UC ONLINE: Berkeley's Multiloop Computer Control Program," *Chem. Eng. Educ.*, **21**(3), 122 (1987).

Gilles, E. D., "Some New Approaches for Controlling Complex Processes in Chemical Engineering," *Proc. Int. Conf. Chem. Proc. Contr.*, 689, Elsevier (1986).

Gould, L. A., *Chemical Process Control: Theory and Applications,* Addison Wesley, Reading, MA (1969).

Gusciora, P. H., "Detecting and Avoiding Unstable Operation of Autothermal Reactors," PhD Thesis, Univ. of California, Berkeley (1986).

Gusciora, P. H., and A. S. Foss, "A Reduced-Order Model of a Fixed-Bed Reactor Based on Novel Application of the Taylor-Dispersion Approximation," Amer. Contr. Conf., Atlanta (1988).

Lappinga, A. J., "Time-Optimal and Internal Model Control of a Feed-Preheat Exchanger and Coordination with Reactor Control," MS Thesis, Univ. of California, Berkeley (1984a).

Lappinga, A. J., and A. S. Foss, "Rapid Set-Point Attainment of Reactor Feed Preheat System and Coordination with Reactor Control," *Proc. Amer. Contr. Conf.*, 1624, San Diego (1984b).

Leonard, D. L., Private Communication (Nov., 1986).

Lewin, D. R., and R. Lavie, "Optimum Operation of a Tube-Cooled Ammonia Converter in the Face of Catalyst Bed Deactivation," *Instn. Chem. Eng. Symp. Ser.*, **87,** 393, Pergammon, London (1984).

Litz, L., "Order Reduction of Linear State-Space Models Via Optimal Approximation of Nondominant Nodes," *Large Scale Systems,* **2,** 171 (1981).

Luenberger, D. G., *Linear and Nonlinear Programming,* 2nd ed., Addison Wesley, Reading, MA (1984).

Luss, D., and N. R. Amundson, "Stability of Loop Reactors," *AIChE J.*, **13,** 279 (1967).

McDermott, P. E., and D. A. Mellichamp, "Pole Placement Self-Tuning Control of Unstable Nonminimum-Phase Systems," *Proc. Am. Contr. Conf.*, 825, San Francisco (1983).

McDermott, P. E., D. A. Mellichamp, and R. G. Rinker, "Multivariable Self-Tuning Control of a Tubular Autothermal Reactor," *Proc. Amer. Contr. Conf.*, 1614, San Diego (1984).

Metchis, S. G., "Averting Extinction in Operating Autothermal Catalytic Reactors," PhD Thesis, Univ. of California, Berkeley (1982).

Metchis, S. G., and A. S. Foss, "Averting Extinction in Autothermal Catalytic Reactor Operations," *AIChE J.*, **33**(8), 1288-1299 (Aug., 1987).

Michelsen, M. L., H. B. Vakil, and A. S. Foss, "State-Space Formulation of Fixed-Bed Reactor Dynamics," *I&EC Fund.*, **12**(3), 323 (Aug., 1973).

Orcutt, J. C., and D. E. Lamb, "Stability of Fixed Bed Catalytic Reactor with Feed-Effluent Heat Exchange," *Autom. and Remote Contr.*, **4,** 274 (1960).

Powell, M. J. D., "A Fast Algorithm for Nonlinearly Constrainted Optimization Calculations," *Lecture Notes in Mathematics,* **630,** Dundee Conf. on Numerical Analysis, Springer-Verlag, New York (1978a).

Powell, M. J. D., "Algorithms for Nonlinear Constraints that use Lagrangian Functions," *Mathematical Programming,* **14**(2), 224 (1978b).

Rosenbrock, H. H., and C. Storey, *Computational Techniques for Chemical Engineers,* Pergamon Press, Oxford, England (1966).

Silva, J. M., "Multi-bed Catalytic Reactor Control Systems: Configuration, Development and Experimental Testing," PhD Thesis, Univ. of California, Berkeley (1978).

Silva, J. M., P. H. Wallman, and A. S. Foss, "Multibed Catalytic Reactor Control Systems: Configuration, Development and Experimental Testing," *I&EC Fund.*, **18**(4), 383 (1979).

Stephens, A. D., and R. J. Richards, "Steady-State and Dynamic Analysis of an Ammonia Synthesis Plant," *Autom.*, **9,** 65 (1973).

van Heerden, C., "Autothermic Processes: Properties and Reactor Design," *Ind. and Eng. Chem.*, **45,** 1242 (1953).

van Heerden, C., "The Character of the Stationary State of Exothermic Processes," *Chem. Eng. Sci.*, **8,** 133 (1958).

Wallman, P. H., "Computer Control of a Fixed-Bed Catalytic Reactor," PhD Thesis, Univ. of California, Berkeley (1977).

Wallman, P. H., J. M. Silva, and A. S. Foss, "Multivariable Integral Controls for Fixed-Bed Reactors," *I&EC Fund.*, **18**(4), 392 (1979).

Wong, C., D. Bonvin, D. A. Mellichamp, and R. G. Rinker, "On Controlling an Autothermal Fixed-Bed Reactor at an Unstable State: IV. Modeling Fitting and Control of the Laboratory Reactor," *Chem. Eng. Sci.*, **38**(4), 619 (1983).

Manuscript received May 11, 1988, and revision received March 1, 1989.